

# Rapid Homogenization of Bi<sub>0.85</sub>Sb<sub>0.15</sub> Alloy by Equal Channel Angular Extrusion

S. Ceresara<sup>1</sup>, G. Giunchi<sup>1</sup>, P. Bassani<sup>2</sup>, T. Cavallin<sup>2</sup>, and C. Fanciulli<sup>3</sup>

<sup>1</sup> EDISON S.p.A, Foro Buonaparte, 31, 20121 Milano, Italy

<sup>2</sup> CNR-IENI, Corso Promessi Sposi, 29, 22053 Lecco, Italy

<sup>3</sup> CNR-INFN LAMIA, Corso Perrone, 24, 16152 Genova, Italy

## Abstract

Equal Channel Angular Extrusion (ECAE) was tested on *as-cast* Bi<sub>0.85</sub>Sb<sub>0.15</sub> alloys of different purity (4N and 5N), with the aim of eliminating microstructure inhomogeneities (Sb segregation on dendrite arms).

The homogeneity degree promoted by hot plastic deformation was monitored by optical microscopy, SEM, X-ray diffraction, differential thermal analysis and electron microprobe analysis.

After 6 ECAE passes at 523 K no trace of dendrites was observable at optical microscope; the micro-homogeneity, however, improved with further increasing the number of passes.

High density material was obtained, with an average grain size of about 20 μm.

In the temperature range of 90 to 300 K, the variation of the Seebeck coefficient of the ECAE processed alloys, prepared from 5N purity starting elements, approaches the behaviour of single crystals of similar composition; at temperatures above 150 K, the figure of merit is higher than in single crystals.

## Introduction

Since half a century, Bi-Sb single crystals are recognized as the best *n*-type thermoelectric material for low temperature (80 K) applications (see reference [1] for a survey). The optimum alloy composition is around Bi<sub>0.85</sub>Sb<sub>0.15</sub>.

Unfortunately, single crystals are brittle, thus limiting low temperature thermoelectric applications. To overcome this problem, the development of polycrystalline materials has been attempted. However, the synthesis of Bi-rich polycrystals poses serious difficulties, since the wide separation of the liquidus and solidus curves in the Bi-Sb phase diagram [2] causes severe Sb segregation on dendritic arms in the *as-cast* material.

So far, powder metallurgy has been the preferred approach [1] for preparing polycrystalline samples. The figure of merit of these materials is considerably lower at temperatures below 100 K with respect to the single crystal, but it can be greater at temperatures above 150 K, up to a factor of two [3].

Among recent results appeared in the literature, annealing of quenched alloys has been proposed [4] for the preparation of polycrystals. Although this process gives acceptable figures of merit, it is not, in our opinion, an industrially viable process, since it requires annealing times of 200 days at 523 K.

In an other recent paper [5], the use of very high pressures, up to 6 GPa is proposed for compacting mechanically alloyed powders; in spite of the significant improvement of the figure of merit, also this process cannot be defined as industry-oriented.

In this work, according to a standard metallurgical practice, we proposed to eliminate dendrite arms in the *as-cast* Bi<sub>0.85</sub>Sb<sub>0.15</sub> alloy by hot plastic deformation. To this goal, the quenched ingot was processed by Equal Channel Angular Extrusion (ECAE).

## Experimental

The ECAE process, first introduced by Segal [6], is sketched in Fig.1. When the sample crosses the channel intersection plane of trace OO', it undergoes a *simple* shear deformation,  $\gamma$ , given by [7]:

$$\gamma = 2 \cot(\phi/2 + \psi/2) + \psi \operatorname{cosec}(\phi/2 + \psi/2) \quad (1)$$

The *equivalent deformation*,  $\varepsilon$ , is given by [7]:

$$\varepsilon = 3^{-0.5} \gamma \quad (2)$$

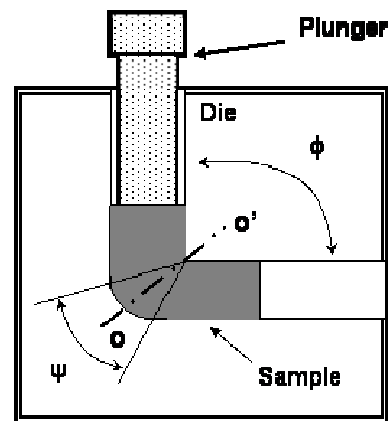


Fig. 1 Scheme of ECAE process.

Our experimental equipment has been described in previous papers [8, 9]. The two channels, 40 mm in diameter, intersect at  $\Phi = 90^\circ$ ; the entry channel is 120 mm in length, whereas the exit channel is 100 mm; the value of the  $\Psi$  angle is  $40^\circ$ , hence the true plastic strain after each pass is  $\varepsilon = 0.98$ . Six heating elements, 500 watt each, enable a uniform temperature in the channels and an accurate control of the extrusion temperature.

Four alloy ingots, with a nominal composition Bi<sub>0.85</sub>Sb<sub>0.15</sub>, were prepared in our laboratory, by melting and mixing the constituent elements, in an evacuated quartz ampoule, at 773 K for 2 hours and water quenching from this temperature. The cast ingots were 12.6 mm in diameter and about 100 g in weight. The nominal purity of the starting materials was 4 N for the ingots n°1 to n° 3, whereas was 5 N for ingot n°4.

Each ingot was subjected to ECAE process, following the same procedures previously experimented for thermoelectric Chalcogenides [8, 9]: cylindrical samples, 12 mm in diameter

and 60 mm in length, were machined from the *as cast* ingots and inserted in the middle of a Cu can, 40 mm in outer diameter and 110 mm in length, with the interposition of a 0.5 mm thick Nb tube as diffusion barrier. Finally, a Cu closure plug was applied.

Ingot n°1 was subjected to 6 ECAE passes at 473 K; ingot n° 2 received 6 ECAE passes at 473 K and 4 additional passes at 523K; ingots n° 3 and n° 4 had 6 and 8 ECAE passes at 523 K, respectively. For all ECAE experiments, the so called *route C* was used, consisting into a 180° rotation of the billet around its long axis at each pass.

Graphite was used as lubricant and the extrusion speed was about 10 mm/min.

After extrusion, the Cu can and Nb barrier were mechanically removed.

Thermoelectric parameters,  $\alpha$ ,  $\rho$ ,  $\lambda$ , were measured in the temperature range of 80 to 300 K, on samples 15 mm long, with a transverse section  $2 \times 3 \text{ mm}^2$  (the long dimension of the samples was parallel to the extrusion direction).

In particular, the Seebeck coefficient,  $\alpha$ , was calculated by the relation  $\alpha = \Delta V / \Delta T$ , where  $\Delta V$  is the voltage difference across the sample, due to a temperature difference,  $\Delta T$ , at its ends; temperature and voltage were measured at the same points, using thermocouples.

The electrical resistivity,  $\rho$ , was measured by the standard 4 points technique, whereas the thermal conductivity,  $\lambda$ , was measured by the absolute axial heat flow method, using the equipment described in reference [10].

Vickers micro-hardness measurements were taken on transverse sections, using a Leitz Miniload equipment, with a test load of 98.1 mN, applied for 15 s.

Micro-homogeneity measurements on polished surfaces were performed by a LEO 1430 SEM, equipped with an EDX model INCA x-sight OXFORD Instruments.

X-ray diffraction patterns were taken by a PANalytical mod. X Pert PRO equipment, using Cu  $K_\alpha$  radiation.

Differential scanning calorimeter analysis was performed by a Q 100 TA Instrument.

## Results and discussion

Ingot n°1, ECAE processed at 473 K, still presented dendrite arms at optical microscope observation, whereas the other ingots, processed at 523 K, appeared homogeneous.

ECAE processed ingots n° 2 and n° 3, prepared from 4 N purity starting materials, presented a maximum Seebeck coefficient at 170 K ( $\alpha = -120 \mu\text{V/K}$  for ingot n° 2 and  $\alpha = -150 \mu\text{V/K}$  for ingot n°3); at lower temperatures,  $\alpha$  continuously decreased in absolute value, becoming positive above 90 K.

A chemical analysis, by I.C.P., of ingots n°2 and n°3, revealed the presence of Al and of Cu, respectively, as the main impurity; hence it can be argued that both elements introduce holes in the  $\text{Bi}_{0.85}\text{Sb}_{0.15}$  alloy.

For this reason, the rest of the results presented here will concern ingot n°4, prepared from 5 N purity starting materials.

Fig. 2, a and b, shows the optical micrographs of the alloy in the *as-quenched* state and after 8 ECAE passes at 523 K, respectively.

It can be seen that the dendrite structure, present after quenching, is completely eliminated after ECAE at 523 K; from Fig. 2b one can estimate the average grain size after ECAE, which is about  $20 \mu\text{m}$ .

Both the absence of dendrite arms, and the grain size value were confirmed by observations at SEM.

The micro-hardness value after ECAE was  $\text{HV} = 47$ , whereas the density was  $9.25 \text{ g/cm}^3$ , say 98% the full density value,  $9.42 \text{ g/cm}^3$ , calculated from the nominal composition of the sample and the cell volume, as determined from the X-ray diffraction pattern (see Fig.5).

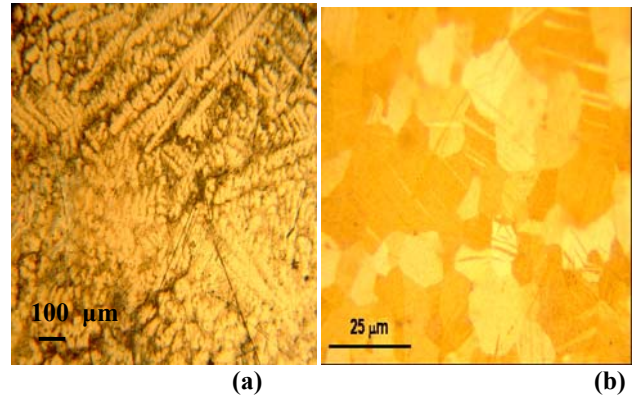


Fig. 2 Optical micrograph of  $\text{Bi}_{0.85}\text{Sb}_{0.15}$  alloy in the *as-quenched* state (a) and after ECAE process at 523 K (b).

Fig. 3 shows the D.S.C. curves for the *as-quenched* and ECAE processed alloy: note that the former presents a first endothermic peak coincident with the melting point of pure Bi, whereas the latter shows a sharp peak, with the inflection point at  $293 \text{ }^\circ\text{C}$ , in agreement with data reported in the literature for a homogeneous Bi-Sb 15 at% alloy [2].

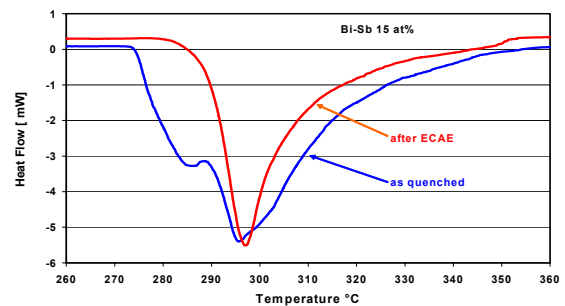


Fig. 3 D.S.C. curves of  $\text{Bi}_{0.85}\text{Sb}_{0.15}$  alloy in the *as-quenched* state and after ECAE process.

X-ray diffraction analysis was performed on both the *as-quenched* and ECAE processed alloy; a comparison of the diffraction patterns is here limited to the (012) peak, as shown in Fig.4.

It is evident that ECAE affects both the position and the sharpness of the peak.

From the complete diffraction pattern of ECAE processed sample, reported in Fig.5, the lattice parameters of the hexagonal cell were calculated as follows:  $a = 4.510 \text{ \AA}$ ,

$c = 11.713 \text{ \AA}$ , in good agreement with data of Cucka and Barrett [11].

The X-ray diffraction pattern of Fig. 5 refers to a transverse section of the extruded bar. By comparing the relative intensities,  $I\%$ , of the peaks with those of pure Bi (pattern JCPDS 85-1331), one can observe that the (104) peak, at about  $38^\circ$ , has  $I = 78\%$ , to be compared with  $I = 34\%$  of the powder standard; this can indicate the presence of a texture in the sample, associated to the process of dynamic recrystallization occurring during ECAE (it is worth noting that the temperature of plastic deformation is 92% the absolute melting temperature of the alloy). The texture, however, is weak, because of the presence of all other (hkl) peaks, with relative intensities resembling the powder pattern.

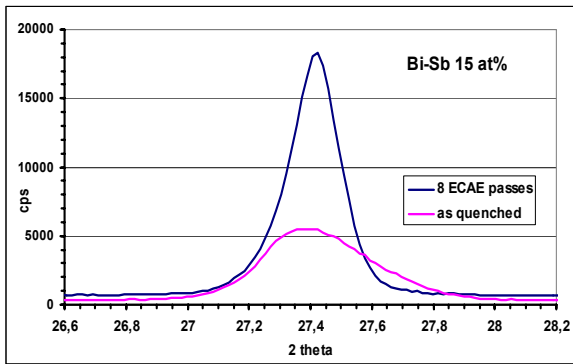


Fig. 4 (012) diffraction peak of  $\text{Bi}_{0.85}\text{Sb}_{0.15}$  alloy in the *as-quenched* state and after ECAE process.

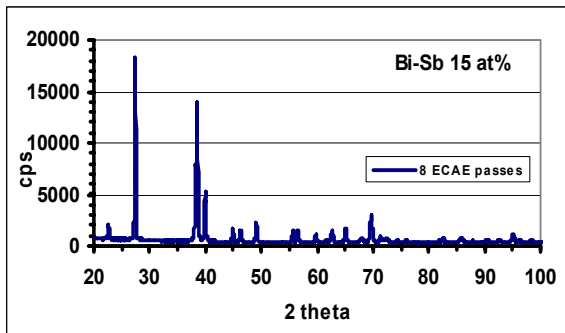


Fig. 5 X-ray diffraction pattern of ECAE processed alloy.

Microprobe analysis was performed on both *as cast* and ECAE processed samples. The standard deviation in composition was  $\pm 12\%$  in the quenched alloy; it decreased to  $\pm 2.4\%$  after 6 ECAE passes at 523 K, and to  $\pm 1.9\%$  after 8 passes.

Obviously, the micro-homogeneity increases with increasing the plastic deformation; however, in view of the results obtained for the thermoelectric properties reported below, we believe that 8 ECAE passes at 523 K represent a satisfactory compromise.

Fig. 7 shows the variation of the Seebeck coefficient,  $\alpha$ , with the temperature. The curve strictly follows the behavior

of  $\alpha$  vs.  $T$  of a single crystal of similar composition (14 at%), as reported in [12].

The variation of the electrical resistivity,  $\rho$ , with the temperature, of ECAE processed alloy, is reported in Fig. 7. The resistivity slightly decreases from room temperature down to 200 K, reflecting the increase of the mobility of the charge carriers; at lower temperatures it progressively increases, due to the freezing of carriers.

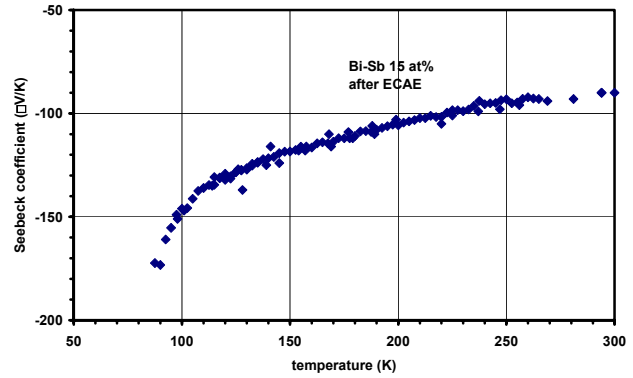


Fig. 6 Seebeck coefficient of ECAE processed alloy.

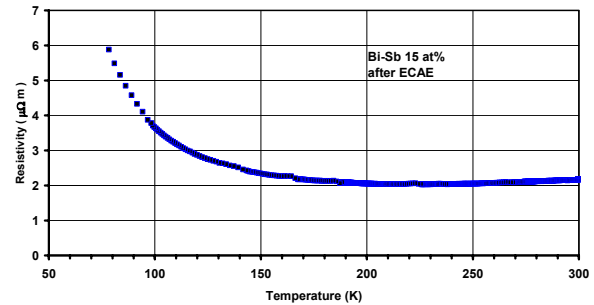


Fig. 7 Electrical resistivity of ECAE processed alloy.

This behavior is qualitatively similar to that of the single crystal [12], but in the latter case the rise in resistivity starts 50 degrees below.

The temperature dependence of the thermal conductivity,  $\lambda$ , is shown in Fig. 8. Values of  $\lambda$  are in this case considerably lower than in single crystal, due to the presence of small grains, with extended boundaries which scatter phonons.

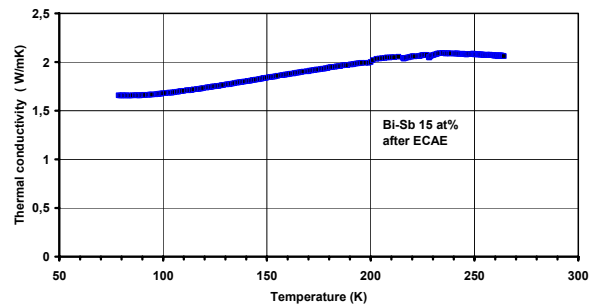


Fig. 8 Thermal conductivity of ECAE processed alloy.

From the above reported values of  $\alpha$ ,  $\rho$  and  $\lambda$ , the figure of merit,  $Z = \alpha^2/\rho \lambda$ , has been computed and reported in Fig. 9, together with the  $Z$  vs.  $T$  curve of the single crystal of similar composition, taken from ref. [12]. As evident, the figure of merit of ECAE processed alloy is higher at all temperatures above 150 K.

A further improvement of the figure of merit is likely possible, by performing some ECAE passes at room temperature (or even lower), after homogenization at 523 K, in order to achieve the same microstructure observed in ECAE processed Chalcogenides [8, 9]: i) sub-micrometric grain morphology, and ii) well defined deformation texture. The former property should guarantee a decrease in thermal conductivity, the latter an increase in electrical conductivity in properly oriented samples.

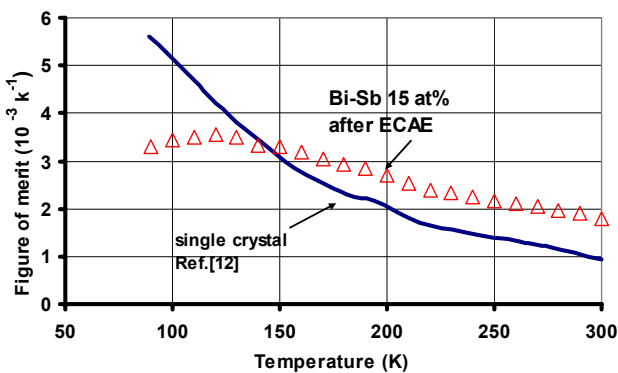


Fig. 9 Figure of merit of ECAE processed alloy.

### Conclusions

Results of the present investigation indicate that ECAE processing of quenched Bi-Sb alloys is a low cost, industrially viable method to obtain a homogeneous thermoelectric material, which, in the temperature range of 150 to 300 K, has a figure of merit higher than in single crystals.

It is emphasized that this novel process of homogenization can be accomplished in a couple of hours; by comparison, homogenization by annealing requires 200 days at 523K [4].

A potential large scale application of this alloy is in the recovery of cold energy of a liquefied natural gas (LNG) plant, through a thermoelectric generator operating between 130 and 290 K [13].

By assuming an average value,  $ZT = 0.8$  [3], for the adimensional figure of merit of the Bi-Sb alloy ( $n$  leg), and by using  $CsBi_4Te_6$  alloy for the  $p$  leg [14], one can easily calculate a conversion efficiency,  $\eta$ , in excess of 11%; by comparison,  $\eta = 9\%$ , if the commercial Chalcogenides are used,  $Bi_{0.5}Sb_{1.5}Te_3$  ( $p$  leg) and  $Bi_2Te_{2.9}Se_{0.1}$  ( $n$  leg) [13].

### Acknowledgments

The Authors are thankful to Mr. G. Ripamonti (EDISON) and to Mr. E. Bassani (CNR IENI) for the assistance in ECAE experiments.

### References

1. Lenoir, B. *et al*, "Bi-Sb Alloys: an Update" *Proc 15<sup>th</sup> International Conference on Thermoelectrics*, Pasadena, March, 1996.
2. Lenoir, B. *et al*, "Growth of  $Bi_{1-x}Sb_x$  Alloys by the Travelling Heater Method", *J. Phys. Chem. Solids*, Vol. 65, No.1, (1995), pp. 99-105.
3. Suse, Y. *et al*, "Structure and thermoelectric properties of  $Bi_{88}Sb_{12}$  ceramics fine particles produced by hydrogen arc plasma" *Proc 12<sup>th</sup> International Conference on Thermoelectrics*, Yokohama, November, 1993, pp. 248-251.
4. Kitagawa, H. *et al*, "Thermoelectric properties of Bi-Sb semiconducting alloys prepared by quenching and annealing" *J. Phys. Chem. Solids*, Vol. 65, No. 7, (2004), pp.1223-1227.
5. Liu, H.J. *et al*, "High-Pressure Preparation and Thermoelectric Properties of  $Bi_{0.85}Sb_{0.15}$  Alloy", *J. Elect. Materials*, Vol. 35, No. 7, (2006), pp. L7-L10.
6. Segal, V. M. "Material processing by simple shear", *Mater. Sci. Eng., A*, Vol. 197, No. 2, (1995), pp. 157-164.
7. Iwahashi, Y. *et al*, "Principles of equal-channel angular pressing for the processing of ultra-fine grained materials", *Scripta Mater.*, Vol. 35, No. 2, (1996), pp. 143-146.
8. Ceresara, S. *et al*, "Microstructure and Thermoelectric Properties in n-Type Chalcogenides processed by Warm ECAE.", *Proc 4<sup>th</sup> European Thermoelectric Conference*, Cardiff, April, 2006.
9. Ceresara, S. *et al*, "Warm ECAE: a Novel Deformation process for optimizing Mechanical and Thermoelectric Properties of Chalcogenides", *Proc 25<sup>th</sup> International Conference on Thermoelectrics*, Vienna, August, 2006.
10. Putti, M. *et al*, "Thermopower measurements of high-temperature superconductors: Experimental artifacts due to applied thermal gradient and a technique for avoiding them", *Phys. Rev. B*, Vol. 58, No. 18, (1998), pp. 12344-12349.
11. Cucka, P. *et al*, "The Crystal Structure of Bi and of Solid Solutions of Pb, Sn, Sb, and Te in Bi", *Acta Cryst.*, Vol. 15, (1962), pp. 865-872.
12. Lenoir, B. *et al*, "Effect of Antimony Content on the Thermoelectric Figure of Merit of  $Bi_{1-x}Sb_x$  Alloys", *J. Phys. Chem Solids*, Vol. 59, No.1, (1998), pp. 129-134.
13. Sun, W. *et al*, "Performance of cryogenic thermoelectric generators in LNG cold energy utilization", *Energ Convers Manag*, Vol. 46, (2005), pp. 789-796.
14. Chung, D.C. *et al*, " $Cs Bi_4 Te_6$ : a high-performance thermoelectric material for low-temperature applications", *Science*, Vol. 287, (2000), pp. 1024-1027.